Title

Improved lipogenesis gene expression in liver is associated with elevated plasma angiotensin 1-7 after AT1 receptor blockade in insulin-resistant OLETF rats

Authors

Godoy-Lugo, Jose A
Mendez, Dora A
Rodriguez, Ruben
et al.

Publication Date

2022-09-01

DOI

10.1016/j.mce.2022.111729

Peer reviewed

Molecular and Cellular Endocrinology 555 (2022) 111729

Contents lists available at ScienceDirect

Molecular and Cellular Endocrinology

journal homepage: www.elsevier.com/locate/mce

Improved lipogenesis gene expression in liver is associated with elevated plasma angiotensin 1-7 after AT1 receptor blockade in insulin-resistant OLETF rats

Jose A. Godoy-Lugo [a,*], Dora A. Mendez [a], Ruben Rodriguez [a], Akira Nishiyama [b], Daisuke Nakano [b], Jose G. Soñanez-Organis [c], Rudy M. Ortiz [a]

[a] School of Natural Sciences, University of California, Merced, CA, USA
[b] Department of Pharmacology, Kagawa University Medical School, Kagawa, Japan
[c] Universidad de Sonora, Departamento de Ciencias Químico Biológicas y Agropecuarias, Navojoa, Sonora, Mexico

ARTICLE INFO

Keywords:
Non-alcoholic fatty liver disease
Angiotensin receptor blocker
Glycolysis
ARB
Glucokinase

ABSTRACT

Increased angiotensin II (Ang II) signaling contributes to insulin resistance and liver steatosis. In addition to ameliorating hypertension, angiotensin receptor blockers (ARBs) improve lipid metabolism and hepatic steatosis, which are impaired with metabolic syndrome (MetS). Chronic blockade of the Ang II receptor type 1 (AT1) increases plasma angiotensin 1-7 (Ang 1–7), which mediates mechanisms counterregulatory to AT1 signaling. Elevated plasma Ang 1–7 is associated with decreased plasma triacylglycerol (TAG), cholesterol, glucose, and insulin; however, the benefits of RAS modulation to prevent non-alcoholic fatty liver disease (NAFLD) are not fully investigated. To better address the relationships among chronic ARB treatment, plasma Ang 1–7, and hepatic steatosis, three groups of 10-week-old-rats were studied: **(1)** untreated lean Long Evans Tokushima Otsuka (LETO), **(2)** untreated Otsuka Long Evans Tokushima Fatty (OLETF), and **(3)** OLETF + ARB (ARB; 10 mg olmesartan/kg/d × 6 weeks). Following overnight fasting, rats underwent an acute glucose load to better understand the dynamic metabolic responses during hepatic steatosis and early MetS. Tissues were collected at baseline (pre-load; T0) and 1 and 2 h post-glucose load. AT1 blockade increased plasma Ang 1–7 and decreased liver lipids, which was associated with decreased fatty acid transporter 5 (FATP5) and fatty acid synthase (FASN) expression. AT1 blockade decreased liver glucose and increased glucokinase (GCK) expression. These results demonstrate that during MetS, overactivation of AT1 promotes hepatic lipid deposition that is stimulated by an acute glucose load and lipogenesis genes, suggesting that the chronic hyperglycemia associated with MetS contributes to fatty liver pathologies via an AT1-mediated mechanism.

1. Introduction

The prevalence of non-alcoholic fatty liver disease (NAFLD) is approximately 12% globally (Ge et al., 2020) and estimated to be as high as 30% in the US and Western countries (Neuschwander-Tetri and Caldwell, 2003). Increased circulating lipids and lipogenesis promote the development of NAFLD, which is an umbrella term that encompasses the spectrum of liver lesions, ranging from simple triacylglycerol (TAG) accumulation to cirrhosis (Paschos and Paletas, 2009). NAFLD is strongly associated with metabolic syndrome (MetS) and its characteristics (Fattahi et al., 2016; Grundy et al., 2005). MetS is a cluster of conditions that can include increased circulating TAG and glucose, adiposity, arterial pressure, which collectively increase the risk of severe cardiovascular and metabolic disease (de Kloet et al., 2010). The renin-angiotensin system (RAS) primarily regulates cardiovascular function and renal hemodynamics. Angiotensin II (Ang II) is the peptide responsible for the majority of the physiological actions of RAS via its type 1 receptor (AT1) (de Kloet et al., 2010). Elevated plasma Ang II and over-activation of AT1 contribute to insulin resistance (Di Pasqua et al., 2022) and fatty liver (Wei et al., 2008). Ang II-mediated activation of AT1 may overload the liver by promoting *de novo* lipogenesis (DNL) (Matthew Morris et al., 2013). Chronic infusion of Ang II in rats increased circulating insulin, non-esterified fatty acids (NEFA), and TAG, and liver TAG synthesis (Ran et al., 2004a, 2005). However, the

* Corresponding author. Department of Molecular & Cell Biology, University of California, Merced, 5200 N Lake Rd., Merced, CA, 95340, USA.
E-mail address: jgodoy4@ucmerced.edu (J.A. Godoy-Lugo).

https://doi.org/10.1016/j.mce.2022.111729
Received 13 January 2022; Received in revised form 18 July 2022; Accepted 21 July 2022
Available online 31 July 2022

mechanisms promoting NAFLD during MetS (Ipsen et al., 2018) in relation to hepatic Ang II signaling (Grundy et al., 2005) have not been completely elucidated.

Angiotensin receptor blockers (ARB) displace Ang II from AT1, its primary receptor (Miura et al., 2011), inhibiting Ang II signaling. While ARBs are widely used to ameliorate MetS-related hypertension (Yamada, 2011), they also improve components of the lipid profile and hepatic lipid accumulation in animals (Kaji et al., 2011; Benson et al., 2004) and humans (Kyvelou et al., 2006; Hanefeld and Abletshauser, 2001). We have previously published the benefits of AT1 blockade on adipose insulin resistance and hyperglycemia (Rodriguez et al., 2021), liver lipid profile of older rats (Godoy-Lugo et al., 2021), and redox response in the heart (Thorwald et al., 2018). However, the mechanisms that promote the metabolic improvements of chronic AT1 blockade on the MetS-associated fatty liver in response to a glucose challenge have not been examined.

Angiotensin 1-7 (Ang 1–7) is another RAS peptide that counter-regulates the adverse effects promoted by elevated Ang II signaling (Jiang et al., 2014). In rats, AT1 blockade increased plasma Ang 1–7 (Reudelhuber, 2006), which decreased plasma TAG, total cholesterol (TC), glucose, and insulin sensitivity (Santos et al., 2010) as well as hepatic gluconeogenesis (GNG) and glycogenolysis (GGL) (Bilman et al., 2012). Ang 1–7 also increased glucose uptake in hepatocytes (Cao et al., 2014) and decreased adipose lipogenesis in rats (Moreira et al., 2017). Conversely, AT1 blockade increased GNG in hyperglycemic hepatocytes (Cho and Cho, 2019). These contrasting data demonstrate the incongruency of the effects of the ARB-induced increase in Ang 1–7 on hepatic lipid metabolism during MetS. (Reudelhuber, 2006).

NAFLD is closely linked to hepatic insulin resistance (Samuel and Shulman, 2018). Hyperinsulinemia may drive NAFLD through increased synthesis of TAG (Nagle et al., 2009), leading to hepatic TAG accumulation, which is hallmark of NAFLD (Ipsen et al., 2018). The rate-limiting enzyme in TAG synthesis is glycerol-3-phosphate acyltransferase (GPAT) (Yu et al., 2018) and the last step of TAG formation is catalyzed by diacylglycerol O-acyltransferase (DGAT) (Yen et al., 2008). Patients with NAFLD present with elevated expression of hepatic GPAT (Arendt et al., 2015). Accordingly, DGAT deficiency protected primary hepatocytes from lipid deposition by decreasing TAG synthesis (Villanueva et al., 2009). Liver TAG can also be incorporated into very-low-density lipoproteins (VLDL) (Perla et al., 2017). Larger VLDL particles that cannot be exported extracellularly can also drive lipid accumulation (Horton et al., 1999; Berger and Moon, 2021). AT1 blockade decreased liver TAG accumulation in Zucker fatty rats (Ran et al., 2004b), while others have reported no change in liver TAG (Rong et al., 2010) suggesting that some aspects of the differences in phenotype may modulate effectiveness of chronic ARB treatment.

Although advances in the studies of Ang II and Ang 1–7 signaling in relation to metabolic improvements in the liver exist, specific examination of the expression of lipid regulating proteins in response to an acute glucose challenge, following chronic AT1 blockade, requires further study. Here, we investigated the impacts of chronic AT1 blockade on circulating Ang 1–7 levels, and their association to changes in hepatic lipogenesis and NAFLD including the dynamic metabolic responses to an acute glucose challenge.

2. Methods

All experimental procedures were reviewed and approved by the institutional animal care and use committees of the Kagawa Medical University (Japan) and the University of California, Merced (USA). This study was designed to assess: **(1)** basal, static effects of chronic AT1 blockade represented by changes at time 0 (T0) and **(2)** acute, dynamic effects of acute hyperglycemia induced by bolus glucose represented by changes in post-glucose load samples. The importance of assessing the acute, dynamic response to glucose is to expand our understanding of the potential impacts of acute hyperglycemia (i.e., post-prandial bout) on the effectiveness of chronic AT1 blockade on hepatic lipid metabolism in response to a nutrient overload. Additionally, this dataset complements our previous studies in the same animals, where we assessed the contribution of AT1 activation in relation to insulin signaling (Rodriguez et al., 2021), cardiac redox biology (Thorwald et al., 2018), and renal function through regulation of inflammation and blood pressure (Rodriguez et al., 2018a). Therefore, previously presented phenotypic data (i.e., body mass, blood pressure, plasma glucose, insulin, glucagon, TAG, NEFA, and liver mass) are included (Table 1) to demonstrate the efficacy of the AT1 blockade and its systemic effects.

2.1. Animals

Age-matched, male, 10-week-old, lean strain-control Long Evans Tokushima Otsuka (LETO; 279 ± 7 g) and obese Otsuka Long Evans Tokushima Fatty (OLETF; 359 ± 3 g) rats (Japan SLC Inc., Hamamatsu, Japan) were used. NAFLD is not progressed at this age in OLETFs (Song et al., 2013), providing the opportunity of examining the conditions during the development of more severe hepatic lipid deposition.

Animals were acclimated to the facility for 1 week before being randomly assigned to permanent cages. Rats were assigned to the following groups (animals/group/time point): **(1)** untreated LETO (n = 5), **(2)** untreated OLETF (n = 8), and **(3)** OLETF + angiotensin receptor blocker (ARB; 10 mg olmesartan/kg/d × 6 weeks; n = 8). Conscious rats were administered ARB (Daiichi-Sankyo, Tokyo, Japan) by oral gavage. ARB was suspended in carboxymethyl cellulose (CMC) and untreated rats were gavaged with CMC only. Animals were maintained in groups of two to three animals per cage and tracked through tail marking and cage card labeling. Animals were given access to water and standard laboratory chow *ad libitum* (MF; Oriental Yeast Corp., Tokyo, Japan) and maintained under controlled temperatures (23–24 °C) and humidity (~55%) with a light-dark cycle of 12-12 h.

Animals were fasted for 12 h ± 15 min. To investigate the dynamic response to a glucose challenge (nutrient overload), animals were sacrificed at baseline (T0, fasting/no glucose) and 1 (T1) and 2 h (T2) after a bolus, glucose load (2 g glucose/kg mass) administered by gavage. Dissection times were staggered to ensure correct timing to correspond with the prescribed timepoints. Trunk blood was collected in vials containing EDTA (Sigma-Aldrich, EDS) and proteinase inhibitor cocktail (Sigma-Aldrich, P2714). Livers were rapidly perfused, weighed, snap-frozen in liquid nitrogen, and stored at −80 °C until analyzed.

2.2. Western blot

A 25 mg aliquot of frozen liver was used for a two-step extraction of cytoplasm and plasma membrane proteins as previously described (Godoy-Lugo et al., 2021). Briefly, tissue was homogenized in phosphate buffer (50 mM potassium phosphates) (Fisher Scientific, P290 and P285) then centrifuged at 15,000×*g*. The recovered supernatant was used to measure cytoplasmic proteins. A resuspension solution (50 mM potassium phosphate buffer + 1% Triton X-100) (Millipore-Sigma, T8787) was added to the pellet, re-homogenized, sonicated, and centrifuged at

Table 1
Mean (±SD) of end-of-study basal measurements.

	LETO	OLETF	ARB
Body mass (g)	366 ± 15	503 ± 9[a]	481 ± 4
Blood pressure (mmHg)	114 ± 3	142 ± 2[a]	120 ± 2[b]
Glucose (mg/dl)	106 ± 7	139 ± 8[a]	120 ± 6[a,b]
Insulin (ng/ml)	0.23 ± 0.03	1.52 ± 0.73[a]	1.53 ± 0.67[a]
Glucagon (pmol/L)	1.9 ± 0.8	3.3 ± 1.3[a]	3.3 ± 1.6[a]
TAG (mg/dl)	59 ± 22	116 ± 8[a]	88 ± 33
NEFA (mEq/L)	0.53 ± 0.3	0.65 ± 0.1	0.71 ± 0.1
Liver mass (g)	10.2 ± 0.6	17.2 ± 1.0[a]	15.3 ± 1.3[a,b]

[a] Significant difference from LETO ($P < 0.05$).
[b] Significant difference from OLETF ($P < 0.05$).

15,000×*g*. This second recovered supernatant was used to measure plasma membrane proteins. All buffers contained 3% protease inhibitor cocktail (Sigma-Aldrich, P2714). Protein concentrations were measured with the Bradford assay (Bio-Rad Laboratories, 5000203). Total protein aliquots (5–15 μg) were resolved in 8–10% Tris- HCL SDS gels. Proteins were electroblotted onto 0.45-μm polyvinyl difluoride (PVDF) membranes (Millipore-Sigma, IPVH00010) using the Mini Gel Tank and Blot Module Set (Invitrogen, NW2000). Membranes were blocked with intercept blocking buffer (Li-Cor, 927–60001, 927–70001). Prior to data gathering, plasma membrane and cytosolic fractions were tested for purity against Na^{+}-K^{+} ATPase (Abcam, ab76020) and α-tubulin (Abcam, ab52866), respectively. For the proteins measured, primary incubations (16 h) were performed with the corresponding antibodies against FATP5 (1:1000; Invitrogen, PA5-42028), apolipoprotein B (ApoB) (1:1000; Thermo Fisher, PA5-86950), and GCK (1:2000; Proteintech, 15629-1-AP). Membranes were then incubated with IRDye 800CW anti-rabbit (Li-Cor, 926–32213) and/or 680RD donkey anti-mouse IgG secondary antibodies (Li-Cor, 926–68072) (diluted 1:20,000). Blots were visualized using the Odyssey system (Li-Cor) and quantified using the Image Studio Lite ver. 5.2 (Li-Cor). Ponceau stain (PS) was used as loading control following the modified Nakamura's method (Nakamura et al., 1985). Briefly, membranes were rinsed with distilled water, followed by incubation with PS solution (0.1 [w/v] Ponceau S powder in 5% [v/v] acetic acid) for 10 min. For visualization, membranes were thoroughly rinsed with distilled water to remove excess stain and resolved clear bands for imaging.

2.3. Biochemical analyses

Glucose (Autokit Glucose, Fujifilm Wako Diagnostics, 997–03001), NEFA (HR Series NEFA-HR, Fujifilm Wako Diagnostics, 999–34691, 995–34791, 991–34891, & 993–35191), and TAG (Triglyceride Colorimetric Assay Kit, Cayman Chemicals, 10010303) were measured using commercially available kits without modification to any of the manufacturer's instructions. Lipids were extracted from the liver using a modified version of the Folch method (Folch et al., 1957). Briefly, 50 mg aliquots of random parts of frozen liver were homogenized into 2 g of sodium sulfate (Fisher Scientific, S415-212). Then, 4 ml of methanol (Fisher Scientific, A412-4) and 8 ml of chloroform (Fisher Scientific, C298-4) were added. The tubes were vortexed and incubated overnight at 4 °C. After incubation, 2.4 ml of 0.7% sodium chloride (Fisher Scientific, S271-3) was added to each tube and incubated 24 h at 4 °C to separate the phases. The supernatant above the chloroform layer was discarded and the leftover content was evaporated in a new tube. When the samples were dry, 0.25 ml of isopropanol (Fisher Scientific, A417-4) was added, the tubes were vortexed, and the homogenous contents transferred into a microcentrifuge tube. All samples were analyzed in duplicate and only values with percent coefficients of variability of less than 10% were accepted.

2.4. Measurements of Ang 1–7 and MAS1

Plasma Ang 1–7 was measured through ELISA (Cloud-Clone Corp, CES085Mi), using 50 μL of EDTA plasma. The Ang 1–7 receptor, proto-oncogene Mas (MAS1), was measured in the plasma membrane fractions of the liver using the Rat MAS1/MAS ELISA (LSBio, LS-F66779) using 5 μL aliquots of the membrane protein extract, equivalent to 20 μg of total membrane protein. All procedures were carried out following the manufacturer's instructions. All samples were analyzed in duplicate and only values with percent coefficients of variability of less than 10% were accepted.

2.5. qPCR

Total RNA was obtained using TRIzol reagent (Invitrogen, 15596026) from 25 mg of random pieces of frozen liver. Genomic DNA was degraded using DNase I enzyme (Roche, 04716728001). Complementary DNA was reverse transcribed from gDNA-free RNA using the High-Capacity cDNA Reverse Transcription Kit (Applied Biosystems, 4368814) using oligo dT. Quantitative PCR reactions were performed including a melting curve and run in duplicate, using an equivalent to 50 ng of RNA per reaction. Specific primers for MAS1, AT1, CD36, FATP5, ACC1, FASN, CPT1A, ACOX1, GPAT4, DGAT1, and GCK were used and beta-2-microglobulin (B2M) served to normalize mRNA levels. The primer sequences used for qPCR analyses are shown in Table 2.

Statistics.

Data was tested for normality using the Shapiro-Wilk test (Ghasemi and Zahediasl, 2012). Correlations were calculated using the Pearson r coefficient (Mukaka, 2012) to better assess changes over time. Area under the curve (AUC) analyses were calculated using the area under the concentration curve in batch designs (Jaki and Wolfsegger, 2009), accounting for all timepoints from T0 to T2. Outliers were detected using the ROUT test (Motulsky and Brown, 2006). In the event an outlier was detected and removed, a single value was replaced using the trimming method (Kwak and Kim, 2017). Means ± SD were compared by ANOVAs and considered significantly different at $p < 0.05$, using the Tukey test. Two-way-ANOVAs were used when analyzing datasets with all timepoints (T0, T1, T2) and groups, comparing intra-temporarily. One--way-ANOVA were employed to analyze AUC data. All comparisons were made using the LETO group as control. Statistical analyses were performed with the GraphPad Prism 9.3.1 software (GraphPad Software).

3. Results

To better recognize the significance of the differences between static (chronic AT1 blockade represented by differences at T0) and dynamic (induced by the acute glucose load) responses, the results were described accordingly (static versus dynamic) within each subheading.

3.1. AT1 blockade increased plasma Ang 1–7 levels & decreased Mas1 membrane abundance

Elevated plasma Ang 1–7 typically counteracts the adverse effects of elevated Ang II signaling (Jiang et al., 2014) via stimulation of the MAS1 receptor (Sahr et al., 2016). Activation of the Ang 1-7-MAS1 axis improved hepatic steatosis (Cao et al., 2016). Therefore, measuring the levels of circulating Ang 1–7 and of hepatic MAS1 abundance may

Table 2
Primers used for qPCR.

Primer name	Sequence	NCBI Reference Sequence
B2M F	ATGGGAAGCCCAACTTCCTC	NM_012512.2
B2M R	ATACATCGGTCTCGGTGGGT	
MAS1 F	AACACATGGGCCTCCCATTC	XM_017588808.1
MAS1 R	AACAGGTAGAGGACCCGCAT	
AT1 F	TCTCAGCTCTGCCACATTCC	NM_030985.4
AT1 R	CGAAATCCACTTGACCTGGTG	
CD36 F	TCATGCCGGTTGGAGACCTA	NM_031561.2
CD36 R	CTTCCTCTGGGTTTTGCACG	
FATP5 F	GCCACACCTCATTTCATCCG	NM_024143.2
FATP5 R	GTTTCGGCCTTGTTGTCCAG	
ACC F	ATTGGGGCTTACCTTGTCCG	NM_022193.1
ACC R	TGCATTATCTGGATGCCCCC	
FASN F	CTGCTGCGGGCCAAGACAG	NM_017332.1
FASN R	GCTGTGGATGATGTTGATGATAG	
CPT1A F	ATTGGCAAGCGGGACCATAG	XM_017588838.1
CPT1A R	TGCAGGAACCAGTAAGGGGA	
Acox1 F	CTCACTCGAAGCCAGCGTTA	NM_017340.2
Acox1 R	TTGAGGCCAACAGGTTCCAC	
GPAT4 F	TACCGTGGTTGGATACCTGC	NM_001047849.1
GPAT4 R	ATCAATGGGCGACGTATGGT	
DGAT1 F	GCTATCCGGACAACCTGACC	NM_053437.1
DGAT1 R	CATCTCAAGAACCCGCCGTA	
GCK F	CGGGAGGCATCTACTCCACA	XM_006251179.4
GCKR	GAACCGGTGGCCTCTAGACA	

provide insight to their potential to ameliorate the AT1-mediated detriments in the liver during the progression of NAFLD.

3.1.1. Static changes

Basal plasma Ang 1–7 levels in ARB were 58% and 80% greater than LETO and OLETF, respectively (Fig. 1A). Hepatic MAS1 expression was 29% and 35% lesser in OLETF and ARB, respectively, than LETO (Fig. 1B). Hepatic MAS1 membrane abundance was 21% and 34% lesser in OLETF and ARB, respectively, than LETO, and ARB was 16% lesser than OLETF (Fig. 1C). Hepatic AT1 expression was 31% lesser in ARB than OLETF (Fig. 1D).

3.1.2. Dynamic changes

During the glucose challenge, plasma Ang 1–7 levels in ARB remained 80% and 90% greater than LETO and OLETF at T1, and 13% and 54% greater than LETO and OLETF, respectively (Fig. 1A). Plasma Ang1-7 AUC was 57% and 81% greater in ARB than LETO and OLETF, respectively (Fig. 1B). At T1, hepatic MAS1 expression was 62% and 45% lesser in ARB than LETO and OLETF, respectively, while at T2, MAS1 expression in OLETF and ARB were 38% and 59% lesser, respectively, than LETO (Fig. 1C). At T1, hepatic MAS1 membrane abundance was 24% and 48% lesser in OLETF and ARB, respectively, than LETO, and abundance in ARB was 32% lesser than OLETF (Fig. 1D). At T2, hepatic membrane MAS1 in OLETF and ARB were 35% and 49% lesser than LETO, and 20% lesser in ARB than OLETF (Fig. 1D). At T1, hepatic AT1 expression was 54% and 50% lesser in ARB than LETO and OLETF, respectively, while at T2, AT1 in OLETF and ARB were 64% and 50% lesser, respectively, than LETO (Fig. 1E). Plasma Ang 1–7 levels in ARB were negatively correlated ($r = -0.995$, $p = 0.043$) overtime, before and during the glucose challenge (Fig. 1A). In all groups, hepatic MAS1 membrane abundance correlated with its gene expression (LETO $r = 0.995$, $p = 0.047$; OLETF $r = 0.997$ and $p = 0.037$; ARB $r = 0.998$ and $p = 0.030$) (Fig. 1F).

Collectively, the data suggest that AT1 blockade increased the levels of Ang 1–7, while decreasing both AT1 and MAS1 receptors suggesting that chronic ARB treatment may sensitize the liver to Ang 1–7 via MAS1 (more hormone and less receptor) while decreasing the potential for AT1-mediated injury.

3.2. AT1 blockade decreased liver NEFA content & hepatic FATP5 and FASN expressions

Hepatic NEFA uptake, which is mainly mediated by CD36 and FATP5 (Kawano and Cohen, 2013), and synthesis through DNL (Lambert et al.,

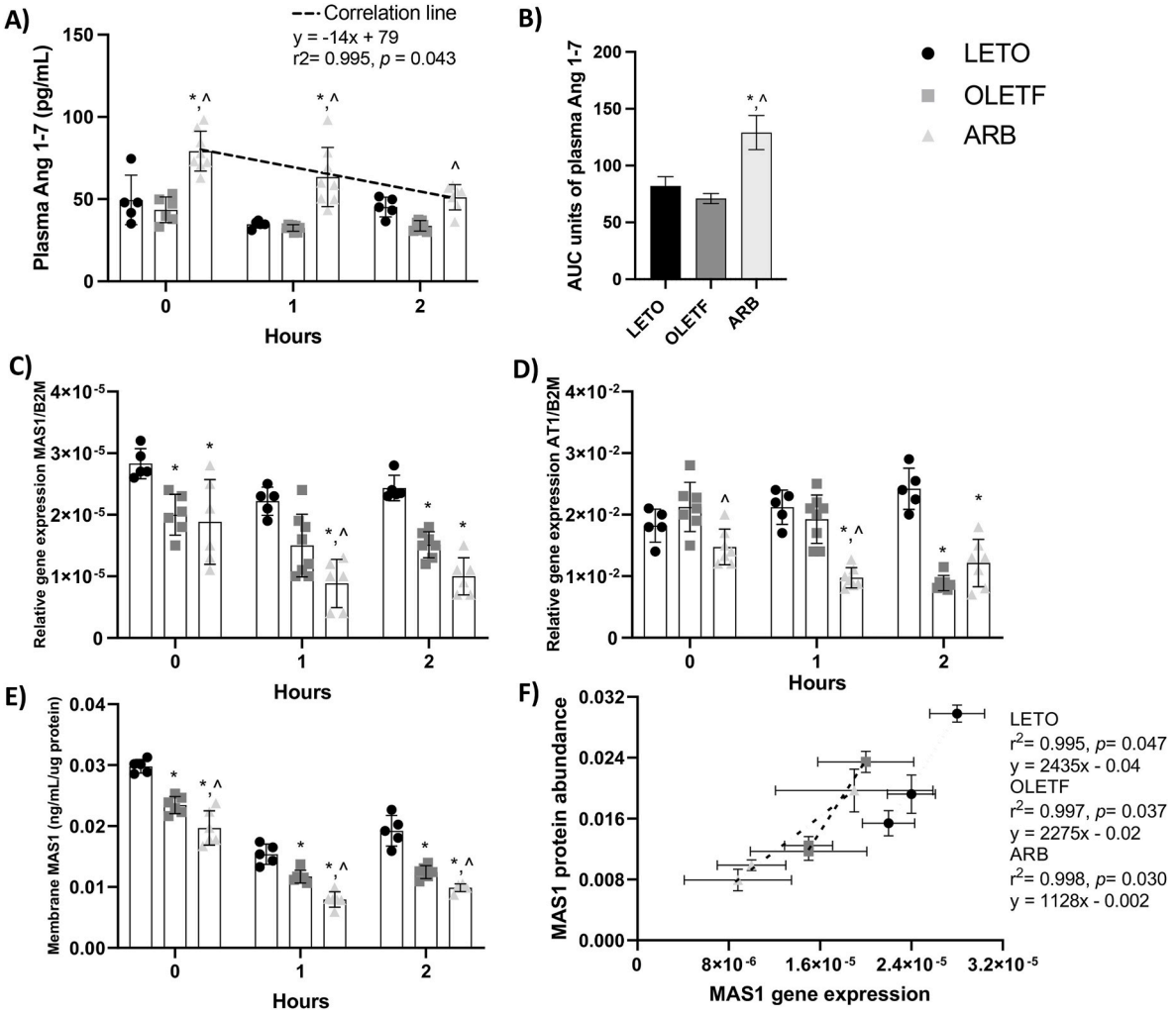

Fig. 1. Increased plasma Ang 1–7 was associated with AT1 blockade. Mean ± SD values for (A) plasma angiotensin 1-7 (Ang 1–7), (B) plasma Ang 1–7 area under the curve (AUC; from T0 to T2), (C) hepatic mRNA expression of Ang 1–7 receptor, MAS1, (D) hepatic mRNA expression of angiotensin II receptor, AT1, (E) hepatic membrane protein expression of MAS1, and (F) correlation between hepatic mRNA expression of MAS1 and hepatic membrane protein abundance during a glucose challenge in Long Evans Tokushima Otsuka (LETO; n = 5), Otsuka Long Evans Tokushima Fatty (OLETF; n = 8), and OLETF + ARB (ARB; n = 8) rats. * *Significant difference from LETO ($P < 0.05$).* ^ *Significant difference from OLETF ($P < 0.05$).*

2014) is increased with NAFLD (Ipsen et al., 2018). Ang II infusion increased hepatic steatosis (Neuschwander-Tetri and Caldwell, 2003), while AT1 blockade (Ran et al., 2004b) increased Ang 1-7-MAS1 axis signaling (Cao et al., 2016) decreasing the steatosis. Moreover, NAFLD can be attenuated by increasing NEFA oxidation (Barbier-Torres et al., 2020). Therefore, measuring the expression of genes related to these pathways during AT1 blockade, and during a glucose challenge, may provide insight about the mechanisms promoting hepatic steatosis during MetS.

3.2.1. Static changes

Basal liver NEFA content in OLETF and ARB were 160% and 112% greater, respectively, than LETO, while levels in ARB were 18% lesser than OLETF (Fig. 2A). Hepatic FATP5 expression in OLETF and ARB was 28% and 51% lesser, respectively, than LETO, and 33% lesser in ARB than OLETF (Fig. 2D). Hepatic ACC expression was 33% lesser in OLETF than LETO (Fig. 2E). Hepatic FASN expression in OLETF and ARB was 30% and 67% lesser, respectively, than LETO, and 53% lesser in ARB than OLETF (Fig. 2F). Hepatic CPT1A expression in OLETF and ARB was 27% and 35% lesser, respectively, than LETO (Fig. 2G). Hepatic ACOX1 expression was 82% greater in OLETF than LETO, while levels were 65% lesser in ARB than OLETF (Fig. 2H). FATP5 protein expression was 20% greater in OLETF than LETO (Fig. 2I).

3.2.2. Dynamic changes

During the glucose challenge, liver NEFA in OLETF and ARB were 78% and 33% greater, respectively, than LETO, while levels in ARB were 25% lesser than OLETF at T1 (Fig. 2A). At T2, levels in OLETF and ARB were 81% and 51% greater, respectively, than LETO, and 17% lesser in ARB than OLETF (Fig. 2A). NEFA AUC in OLETF and ARB was 88% and 49% greater, respectively, than LETO, and 21% lesser in ARB than OLETF (Fig. 2B). At T2, hepatic CD36 expression in OLETF was 132% greater than LETO, and 65% lesser in ARB than OLETF (Fig. 2C). At T1, hepatic FATP5 expression in ARB was 63% and 54% lesser in ARB than LETO and OLETF, respectively, (Fig. 2D). At T2, levels in OLETF and ARB were 22% and 64%, respectively, lesser than LETO, and 53% lesser in ARB than OLETF (Fig. 2D). At T1, hepatic ACC expression in OLETF was 74% greater than LETO, and 42% and 67% lesser in ARB than LETO and OLETF, respectively (Fig. 2E). At T2, levels in OLETF were 51% greater than LETO, and 29% and 53% lesser in ARB than LETO and OLETF, respectively (Fig. 2E). At T1, hepatic FASN expression in OLETF was 88% greater than LETO, and 53% lesser in ARB than OLETF (Fig. 2F). At T2, levels in OLETF were 15% greater than LETO, and 74% and 77% lesser in ARB than LETO and OLETF, respectively (Fig. 2F). Hepatic FASN expression in OLETF correlated positively over time ($r = 0.997$, $p = 0.036$), before and during the glucose challenge (Fig. 2F). At T1, hepatic CPT1 expression in OLETF and ARB was 58% and 78% lesser, respectively, than LETO, and 47% lesser in ARB than OLETF (Fig. 2G). At T2, levels in ARB were 45% and 49% lesser than LETO and OLETF, respectively (Fig. 2G). At T1, hepatic ACOX1 expression in OLETF was 26% greater than LETO, and 70% and 76% lesser in ARB than LETO and OLETF, respectively (Fig. 2H). At T2, levels in OLETF and ARB were 80% and 88% lesser, respectively, than LETO (Fig. 2H). At T1, hepatic FATP5 protein expression was 23% lesser in ARB than OLETF (Fig. 2I). At T2, levels in OLETF were 34% greater than LETO, while levels in ARB remained 22% lesser than OLETF (Fig. 2I).

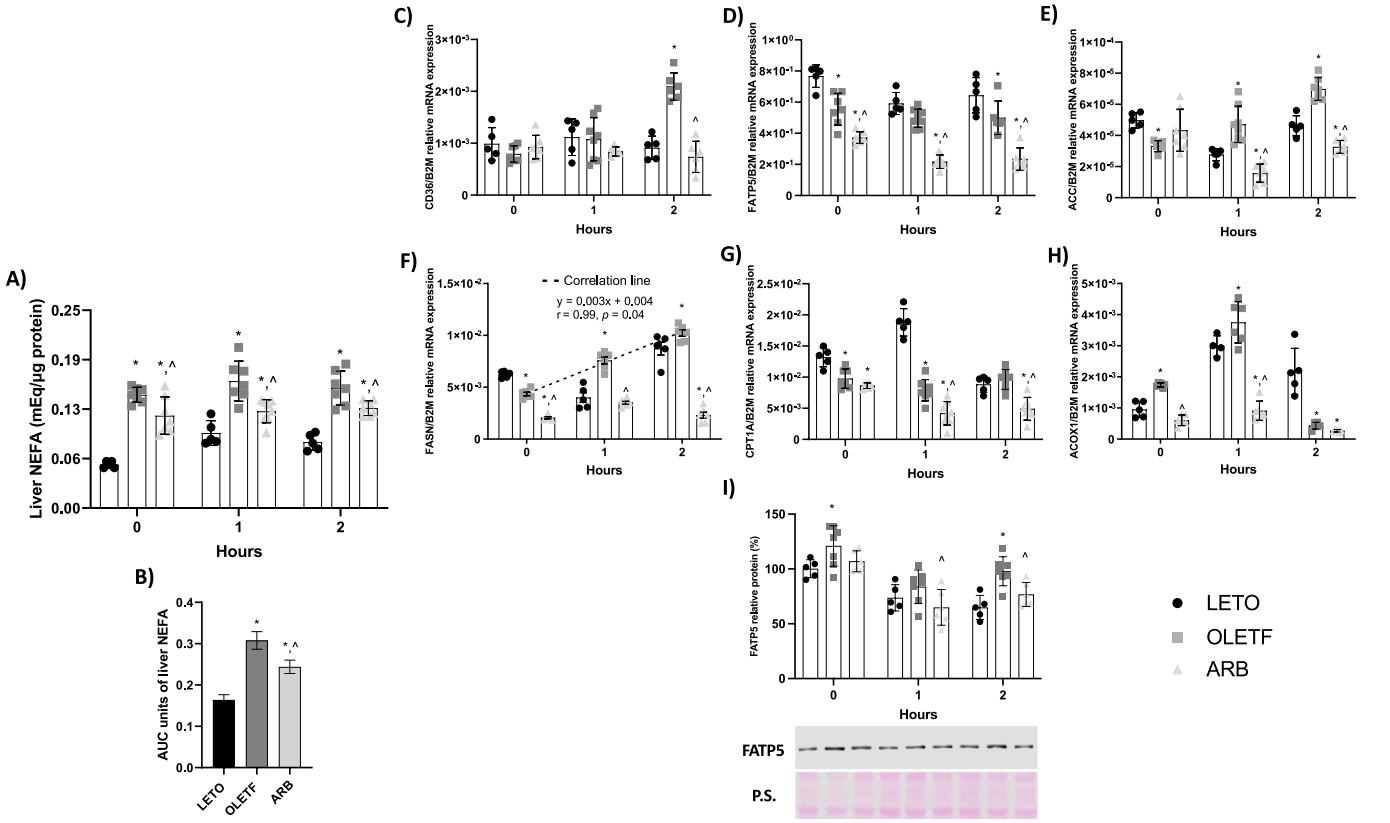

Fig. 2. AT1 blockade decreased basal expression of genes promoting fatty acid uptake and fatty acid synthesis. Mean ± SD values for (A) liver non-esterified fatty acids (NEFA), (B) liver NEFA area under the curve (AUC; from T0 to T2), (C) hepatic mRNA expression of cluster of differentiation 36 (CD36), (D) hepatic mRNA expression of fatty acid transporter 5 (FATP5), (E) hepatic mRNA expression of acetyl-coA carboxylase 1 (ACC), (F) hepatic mRNA expression of fatty acid synthase (FASN), (G) hepatic mRNA expression of carnitine palmitoyltransferase 1A (CPT1A), (H) hepatic mRNA expression of acyl-coA oxidase 1 (ACOX1), and (I) hepatic protein expression of FATP5 during a glucose challenge in Long Evans Tokushima Otsuka (LETO; n = 5), Otsuka Long Evans Tokushima Fatty (OLETF; n = 8), and OLETF + ARB (ARB; n = 8) rats. * *Significant difference from LETO ($P < 0.05$).* ^ *Significant difference from OLETF ($P < 0.05$).*

These data suggest that over-activation of AT1 promotes liver NEFA content by increasing their uptake and synthesis through increased FATP5 and FASN expressions without decreasing their oxidation as supported by the increased expressions of CPT1A and ACOX1 in OLETF. Additionally, these mechanisms may help upregulate DNL during nutrient overload as suggested by the increase in FASN and ACC expressions during the acute challenge and their reciprocal decreases with ARB.

3.3. AT1 blockade decreased basal hepatic TAG and decreased genes of TAG synthesis during the glucose challenge

TAG accumulation in the liver is the hallmark of NAFLD (Ipsen et al., 2018). TAG synthesis in the liver is initiated by GPAT, while DGAT catalyzes the last step to create new TAG (Yu et al., 2018; Yen et al., 2008). TAG can be transported outside of the liver as VLDL cholesterol, formed over a backbone of ApoB (Perla et al., 2017). AT1 blockade (Ran et al., 2004b) and increased Ang 1–7 signaling (Cao et al., 2016) have demonstrated benefits in decreasing hepatic TAG. Thus, measuring liver TAG levels, and the expression of genes for enzymes responsible for TAG synthesis and export during AT1 blockade, and after a glucose load, may provide further insight into the mechanisms involved in the improvements on hepatic TAG accumulation, and the detriments of nutrient overload derived from the glucose challenge.

3.3.1. Static changes

Basal liver TAG in OLETF and ARB were 125% and 79% greater, respectively, than LETO, and 20% lesser in ARB than OLETF (Fig. 3A). Hepatic mRNA expressions of GPAT4 (Fig. 3C) and DGAT1 (Fig. 3D) in ARB were 32% and 36% greater, respectively, than LETO. There were no detectable differences in hepatic ApoB protein expression among the groups at baseline (T0) (Fig. 3E).

3.3.2. Dynamic changes

During the glucose challenge, liver TAG levels in OLETF and ARB were 40% and 32% greater, respectively, than LETO at T2 (Fig. 3A). TAG AUC in OLETF and ARB was 37% and 25% greater than LETO, and 8% lesser in ARB than OLETF (Fig. 3B). At T1, hepatic GPAT4 expression in OLETF and ARB was 37% and 43% lesser, respectively, than LETO (Fig. 3C). At T2, levels in OLETF were 43% greater than LETO and 43% lesser in ARB than OLETF (Fig. 3C). At T1, hepatic DGAT1 expression in OLETF was 65% greater than LETO, and 32% lesser in ARB than OLETF (Fig. 3D). At T2, levels were 64% and 59% lesser in ARB than LETO and OLETF, respectively (Fig. 3D). Hepatic DGAT1 expression in ARB correlated negatively over time ($r = -0.996$, $p = 0.039$) before and during the glucose challenge (Fig. 3D). At T1, hepatic ApoB protein expression was 130% greater in OLETF than LETO, while ARB was 72% lesser than OLETF (Fig. 3E). At T2, OLETF and ARB were 140% and 117% greater, respectively, than LETO (Fig. 3E).

These data suggest that over-activation of AT1 contributes to the accumulation of TAG in the liver during the early phase of MetS. This early manifestation of NAFLD may be partially stimulated by increased TAG synthesis during nutrient overload, more so than during the fasted state, as suggested by the increase in hepatic GPAT4 at T2 and the linear decrease of DGAT1 in the ARB group.

3.4. AT1 blockade increased GCK expression and reduced hepatic glucose levels

Glucokinase (GCK) regulates hepatic glucose disposition and its metabolism (Peter et al., 2011). Ang 1–7 signaling improved insulin signaling (Cao et al., 2014) suggesting its potential to contribute to glucose metabolism. Thus, given the relationship between AT1 blockade and increased plasma Ang 1–7 levels (Reudelhuber, 2006), changes in hepatic glucose and GCK expression may help to better understand hepatic glucose sensitivity after chronic AT1 blockade and in response to a nutrient overload.

3.4.1. Static changes

Basal liver glucose in OLETF and ARB was 137% and 58% greater, respectively, than LETO, and 33% lesser in ARB than OLETF (Fig. 4A). Hepatic GCK expression in ARB was 70% and 97% greater than LETO

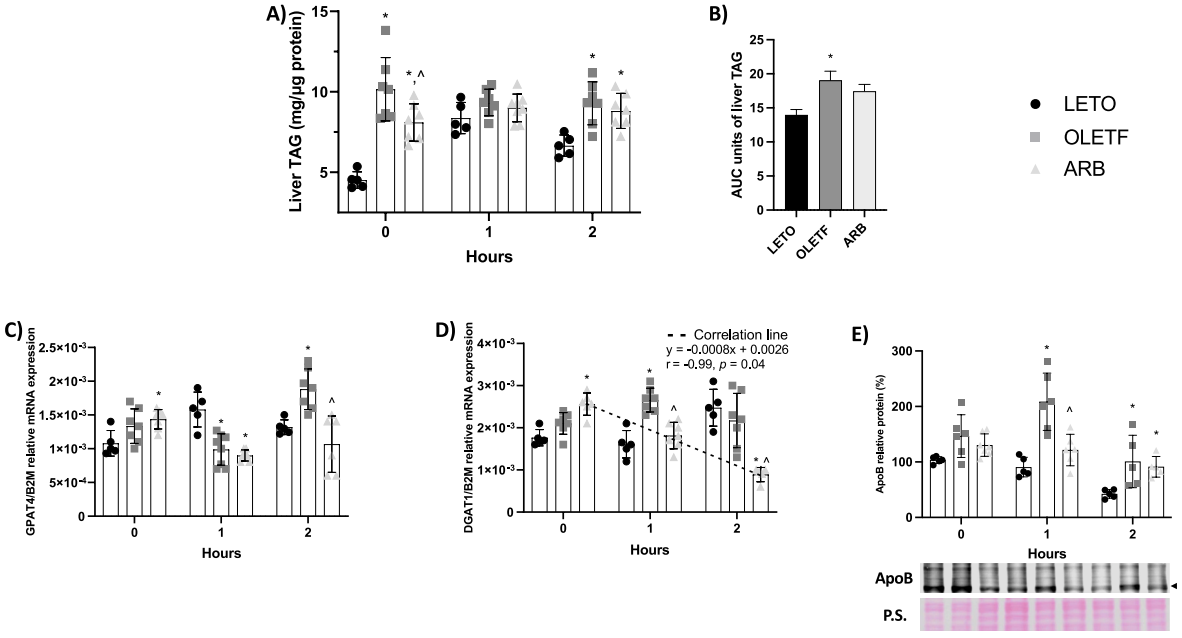

Fig. 3. AT1 blockade decreased basal TAG levels and the expression of TAG synthesis genes. Mean ± SD values for (A) liver triacylglycerol (TAG), (B) liver TAG area under the curve (AUC; from T0 to T2), (C) hepatic mRNA expression of glycerol-3-phosphate acyltransferase 4 (GPAT4), (D) hepatic mRNA expression of diacylglycerol O-acyltransferase 1 (DGAT1), and (E) protein expression of hepatic apolipoprotein B (ApoB) during a glucose challenge in Long Evans Tokushima Otsuka (LETO; n = 5), Otsuka Long Evans Tokushima Fatty (OLETF; n = 8), and OLETF + ARB (ARB; n = 8) rats. * *Significant difference from LETO ($P < 0.05$).* ^ *Significant difference from OLETF ($P < 0.05$).*

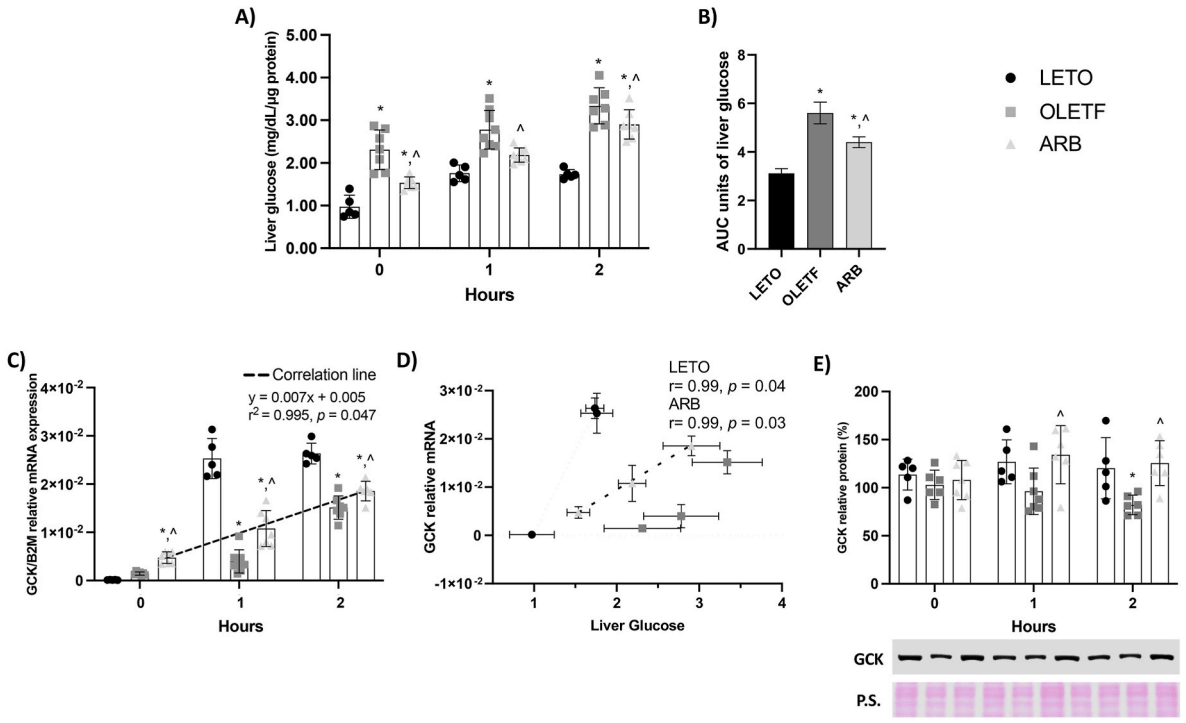

Fig. 4. AT1 blockade increased GCK expression and decreased hepatic glucose levels. Mean ± SD values for (A) liver glucose, (B) liver glucose area under the curve (AUC; from T0 to T2), (C) hepatic mRNA expression of glucokinase (GCK), (D) correlation between liver glucose and hepatic GCK gene expression, and (E) hepatic GCK protein expression during a glucose challenge in Long Evans Tokushima Otsuka (LETO; n = 5), Otsuka Long Evans Tokushima Fatty (OLETF; n = 8), and OLETF + ARB (ARB; n = 8) rats. * *Significant difference from LETO (P < 0.05).* ^ *Significant difference from OLETF (P < 0.05).*

and OLETF, respectively (Fig. 4C).

3.4.2. Dynamic changes

During the glucose challenge, liver glucose in OLETF was 59% greater than LETO and 21% lesser in ARB than OLETF at T1 (Fig. 4A). At T2, levels in OLETF and ARB were 92% and 15% greater, respectively, than LETO, and 40% lesser in ARB than OLETF (Fig. 4A). Glucose AUC in OLETF and ARB was 80% and 41% greater, respectively, than LETO, and 21% lesser in ARB than OLETF (Fig. 4B). At T1, hepatic GCK expression in OLETF and ARB was 88% and 57% lesser, respectively, than LETO, and 150% greater in ARB than OLETF (Fig. 4C). At T2, levels in OLETF and ARB were 73% and 29% lesser, respectively, than LETO, and 23% greater in ARB than OLETF (Fig. 4C). Hepatic GCK expression in ARB correlated positively over time ($r = 0.995$, $p = 0.047$) before and during the glucose challenge (Fig. 4C). Additionally, basal expression levels correlated with liver glucose in LETO ($r = 0.996$, $p = 0.039$) and ARB ($r = 0.998$, $p = 0.028$) but not in OLETF (Fig. 4D). At T1, hepatic GCK protein expression was 40% greater in ARB than OLETF (Fig. 4E). At T2, hepatic GCK in OLETF was 32% lesser than LETO, while ARB was 34% greater than OLETF (Fig. 4E).

These data suggest that over-activation of AT1 may contribute to impaired hepatic glucose metabolism in part by suppressing GCK expression statically and dynamically in response to a post-prandial excursion in glucose. This is further supported by the linear increase of GCK over time and the correlation found in LETO and ARB between GCK expression and liver glucose content before and during the glucose challenge but not in OLETF.

4. Discussion

Elevated RAS, characterized by increased plasma Ang II (Li et al., 2019) and over-activation of the Ang II receptor, AT1 (Fattahi et al., 2016), contributes to the development of NAFLD. Conversely, Ang 1–7 mediates a counter-regulatory mechanism to ameliorate the adverse effects of elevated Ang II signaling (Jiang et al., 2014). In this study, plasma Ang 1–7 was increased statically with chronic AT1 blockade and associated with improved hepatic metabolism. Liver TAG accumulation is the hallmark of NAFLD (Ipsen et al., 2018) and the dysregulation of its synthesis, oxidation, secretion, and storage lead to NAFLD development. Chronic AT1 blockade decreased the expression of hepatic genes and proteins of lipogenesis and lipid transport, basally and during the glucose load. Additionally, chronic AT1 blockade potentially improved the response of the liver to glucose suggested by the increased expression of GCK and decrease of liver glucose content in response to the acute challenge. These novel results support the contention that elevated RAS and overaction of hepatic AT1 promote the manifestation of NAFLD during MetS by impairing both hepatic glucose and lipid metabolism.

Chronic blockade of AT1 by ARBs results in an increase in plasma Ang II because of its displacement from its receptor (Thorwald et al., 2018). The increased levels of plasma Ang 1–7 in the present study, therefore, may be due to an increased availability of Ang II in circulation that is converted to Ang 1–7 via angiotensin converting enzyme 2 (ACE2) as opposed to the traditional pathway from Ang I converted by neprilysin (NEP) (Reudelhuber, 2006) (Patel et al., 2016). Although plasma Ang 1–7 was elevated statically with AT1 blockade, and remained greater than OLETF despite decreasing with the glucose challenge, the abundance of its membrane receptor, MAS1, was decreased. This may be due to AT1 blockade not changing MAS1 expression during the early stages of the ARB treatment (Sukumaran et al., 2011), suggesting that chronic blockade increased the sensitivity of MAS1 to Ang 1–7 as part of the adaptation to an improved metabolic state in the liver (Amato et al., 2016), promoting substrate homeostasis via increased levels of plasma Ang 1–7 (Chandarlapaty, 2012). Alternatively, maintained MAS1 receptor expression is often reported with increased Ang 1–7 through infusion (Abuohashish et al., 2017), which may not mimic the Ang 1–7 increase mediated by AT1 blockade. Increased circulating Ang 1–7 alone may suffice to stimulate pathway signaling (Santos et al., 2010, 2012). Finally, Ang 1–7 signaling may be

suppressed during pathological conditions, which may explain the lack of changes in plasma Ang 1–7 in OLETF (Dias-Peixoto et al., 2012) and the increase in basal plasma and AUC levels of Ang 1–7 with AT1 blockade. Regardless, we caution the interpretation of the results based on the lack of profound changes in MAS1 receptor protein alone. The accurate detection of the MAS1 receptor is controversial, as the available antibodies may still detect bands in MAS1 KO animals (Burghi et al., 2017). For that reason, we measured MAS1 protein by an ELISA, which we validated to help ameliorate this concern. Additionally, we demonstrated that the basal levels of MAS1 gene expression and protein abundance (by ELISA) were correlated in each group, supporting the validity of the MAS1 levels. Regardless, the increased levels of plasma Ang 1–7 despite the lack of increased receptor (MAS1) may be sufficient to contribute to the beneficial effects produced by AT1 blockade (Bilman et al., 2012). Chronic AT1 blockade decreased AT1 expression in the vasculature (Diep et al., 2002) similar to that shown here in the liver, and levels of expression remained decreased in response to the glucose challenge suggesting that ARB treatment may desensitize tissues to excursions in glucose such as during post-prandial nutrient loads.

Hepatic NEFA uptake is increased during NAFLD (Ipsen et al., 2018). In this study, the decrease in liver NEFA associated with chronic AT1 blockade may be derived from decreased FATP5, a principal transporter of NEFA in the liver (Kawano and Cohen, 2013). Additionally, the decrease in CD36 with AT1 blockade at the end of the glucose challenge may demonstrate how the liver is protected by chronic ARB treatment from excessive NEFA accumulation after a nutrient overload (e.g., glucose challenge) (Wilson et al., 2016). Accordingly, the liver can produce NEFA through DNL (Lambert et al., 2014). The increase in liver NEFA AUC in OLETF may result from increased FASN and ACC (Knebel et al., 2019). AT1 blockade decreased FASN expression, while ACC expression was only decreased during the glucose challenge. These data suggest that AT1 activation may contribute to hepatic steatosis during of MetS progression by upregulating DNL.

Conversely, increased NEFA oxidation may not contribute significantly to the decrease in liver NEFA content. Chronic AT1 blockade statically decreased basal hepatic ACOX1 expression, and both ACOX1 and CPT1A expressions were decreased during the glucose challenge suggesting that the potential to increase NEFA oxidation was decreased at this stage. This decrease could also reflect a shift from NEFA to glucose oxidation (Muoio and Newgard, 2008), which may reflect improved glucose utilization following chronic AT1 blockade. Collectively, these results suggest that over-activation of AT1 may contribute to increased hepatic steatosis by increasing NEFA uptake and DNL, ultimately promoting the accumulation of TAG in the liver by increasing the pool of available NEFA.

Increased TAG synthesis and accumulation are the primary mechanisms for inducing and sustaining NAFLD (Nagle et al., 2009). The decrease in hepatic GPAT4 and DGAT1 expressions in ARB following the glucose challenge provides strong support for AT1 activation contributing to the accumulation of hepatic TAG despite the lack of static and dynamic increases in the expression of these enzymes. With chronic blockade of AT1, DGAT1 expression decreased linearly overtime after the glucose load, while GPAT4 decreased only after 2 h. This suggest that the decrease in TAG production during the glucose load may reflect changes in nutrient processing by the liver (Muoio and Newgard, 2008). OLETF rats are characterized by hyperphagia associated with greater meal sizes rather than increased bouts of food intake (Moran, 2008), repeatedly generating nutrient overloads. Thus, chronic blockade of AT1 may be more effective at ameliorating the associated dysregulated metabolism during increased meal-size hyperphagia. Chronic AT1 blockade also decreased ApoB during the glucose load suggesting that VLDL production was not increased. Collectively, these results demonstrate that overactivation of AT1 may increase hepatic TAG synthesis by maintaining transcription of rate-limiting enzymes, while chronic blockade of AT1 sensitizes the transcription of these enzymes to glucose, resulting in decreased expression to prevent the post-prandial accumulation of hepatic TAG especially following extreme carbohydrate overload.

Increased circulating Ang 1–7 improves glucose metabolism (Santos et al., 2010; Echeverria-Rodriguez et al., 2014). Hyperglycemia can indirectly contribute to the development of NAFLD by increasing NEFA synthesis, consequentially impairing their oxidation due to the presence of abundant lipids (Dixon et al., 2001). In our previous studies, AT1 blockade decreased plasma insulin (Rodriguez et al., 2021; Thorwald et al., 2018) and its response to a glucose load (Rodriguez et al., 2018b) associated with increased phosphorylation of the insulin receptor (p-IR) and translocation of Glut4 in adipose (Rodriguez et al., 2021). Accordingly, AT1 blockade also decreased the expression of gluconeogenic genes, which may sensitize the liver to extreme excursions in post-prandial glucose to reduce endogenous glucose production and contribute to systemic glucose homeostasis (Rodriguez et al., 2021). Increased GCK activity regulates hepatic glucose production (Peter et al., 2011) and increased insulin may induce hepatic GCK activity (Sternisha and Miller, 2019), which is decreased in obese, diabetic subjects (Caro et al., 1995). In our study, GCK expression increased with AT1 blockade suggesting that the overactivation of AT1, associated with MetS, decreased the potential of GCK activity. Furthermore, GCK gene expression correlated positively with hepatic glucose levels in both LETO (lean, strain control) and ARB groups. The similarity in this behavior between these two groups suggests that overactivation of AT1 contributes impaired hepatic glucose tolerance. These results further suggest that chronic AT1 blockade may improve hepatic glucose metabolism (i.e., reduced uptake and increase oxidation) during conditions of glucose intolerance, which may partly decrease systemic hyperglycemia and improve insulin resistance.

The contributions of the Ang 1-7-MAS1 axis to the regulation of cellular metabolism in the prevention and amelioration of NAFLD associated with MetS warrant further investigation, as a paucity of data exists on the relations between substrate metabolism and this axis. Increasing plasma Ang 1–7 and MAS1 receptor activation can improve liver fibrosis (Lubel et al., 2009), fat mass (Santos et al., 2010, 2012), increased insulin secretion (Sahr et al., 2016), and insulin response in various tissues (adipose, cardiac, skeletal muscle, and liver) (Rajapaksha et al., 2021). Thus, chronic blockade of AT1 alone may exert beneficial effects similar to those induced by up-regulation of the Ang 1-7-MAS1 axis. Alternatively, the benefits realized by chronic blockade of AT1 may be synergistic with ARB-induced up-regulation of Ang 1–7. However, studies have reported a lack of AT1 blockade-mediated benefits associated with increased Ang 1-7-MAS1 axis signaling. Thus, both mechanisms may stimulate metabolic benefits independently, although in the present study, we suspect the benefits on improvements in liver health and metabolism are likely synergistic.

In summary, our results demonstrating profound improvements in hepatic substrate metabolism especially during an acute glucose challenge with chronic blockade of AT1 suggest that overactivation of AT1 contributes to the manifestation of hepatic steatosis during the early phase of MetS. Among the mechanisms by which AT1 promotes NAFLD include suppression of plasma Ang 1–7, and increased sequestration of hepatic NEFA and synthesis of hepatic TAG. Notably, these improvements were independent of increases in MAS1 receptor expression or membrane abundance, suggesting that the sensitivity of the receptor may be increased with chronic blockade of AT1. Over-activation of hepatic AT1 may contribute significantly to the impaired substrate metabolism associated with NAFLD during MetS. Additionally, chronic AT1 blockade may sensitize the liver to increases in glucose that are common with high glucose meals.

Declarations

Ethics approval and consent to participate: All experimental procedures were reviewed and approved by the institutional animal care and use committees of the Kagawa Medical University (Japan) and the

University of California, Merced (USA).

Consent for publication: Not applicable.

Availability of data and materials: Associated data and materials are available upon reasonable request.

Competing interests: The authors have no relevant financial or non-financial interests to disclose.

Funding: Research was partially funded by University of California Mexico-United States (UC MEXUS) grant 19-194. JAGL was supported by the UC-MEXUS and the Consejo Nacional de Ciencia y Tecnologia (CONACYT) fellowship. JAGL and RR were supported by internal funding from University of California, Merced and by NIH NCMHD9T37MD001480.

CRediT authorship contribution statement

Jose A. Godoy-Lugo: Conceptualization, Project administration, Supervision, Investigation, Data curation, Writing – original draft, preparation, Writing – review & editing. **Dora A. Mendez:** Investigation. **Ruben Rodriguez:** Conceptualization, Project administration, Supervision, Writing – review & editing. **Akira Nishiyama:** Conceptualization, Project administration, Supervision, Writing – review & editing. **Daisuke Nakano:** Conceptualization, Project administration, Supervision, Writing – review & editing. **Jose G. Soñanez-Organis:** Conceptualization, Project administration, Supervision, Writing – review & editing, Funding acquisition. **Rudy M. Ortiz:** Conceptualization, Project administration, Supervision, Data curation, Writing – review & editing, Funding acquisition.

Data availability

Data will be made available on request.

Acknowledgements

We would like to thank G.G.L.R. for their support during the study, and Daiichi-Sankyo (Tokyo, Japan) for their donation of olmesartan to Dr. A. Nishiyama.

Appendix A. Supplementary data

Supplementary data to this article can be found online at https://doi.org/10.1016/j.mce.2022.111729.

References

Abuohashish, H.M., et al., 2017. Angiotensin (1-7) ameliorates the structural and biochemical alterations of ovariectomy-induced osteoporosis in rats via activation of ACE-2/Mas receptor axis. Sci. Rep. 7 (1), 2293.
Amato, D., et al., 2016. Role of angiotensin-(1-7) on renal hypertrophy in streptozotocin-induced diabetes mellitus. Pharmacol. Pharm. 7 (9), 379–395.
Arendt, B.M., et al., 2015. Altered hepatic gene expression in nonalcoholic fatty liver disease is associated with lower hepatic n-3 and n-6 polyunsaturated fatty acids. Hepatology 61 (5), 1565–1578.
Barbier-Torres, L., et al., 2020. Silencing hepatic MCJ attenuates non-alcoholic fatty liver disease (NAFLD) by increasing mitochondrial fatty acid oxidation. Nat. Commun. 11 (1), 3360.
Benson, S.C., et al., 2004. Identification of telmisartan as a unique angiotensin II receptor antagonist with selective PPARgamma-modulating activity. Hypertension 43 (5), 993–1002.
Berger, J.M., Moon, Y.A., 2021. Increased hepatic lipogenesis elevates liver cholesterol content. Mol. Cell 44 (2), 116–125.
Bilman, V., et al., 2012. Decreased hepatic gluconeogenesis in transgenic rats with increased circulating angiotensin-(1-7). Peptides 37 (2), 247–251.
Burghi, V., et al., 2017. Validation of commercial Mas receptor antibodies for utilization in Western Blotting, immunofluorescence and immunohistochemistry studies. PLoS One 12 (8), e0183278.
Cao, X., et al., 2014. The ACE2/Ang-(1-7)/Mas axis can inhibit hepatic insulin resistance. Mol. Cell. Endocrinol. 393 (1–2), 30–38.
Cao, X., et al., 2016. Angiotensin-converting enzyme 2/angiotensin-(1-7)/Mas axis activates Akt signaling to ameliorate hepatic steatosis. Sci. Rep. 6, 21592.
Caro, J.F., et al., 1995. Liver glucokinase: decreased activity in patients with type II diabetes. Horm. Metab. Res. 27 (1), 19–22.
Chandarlapaty, S., 2012. Negative feedback and adaptive resistance to the targeted therapy of cancer. Cancer Discov. 2 (4), 311–319.
Cho, K.W., Cho, D.H., 2019. Telmisartan increases hepatic glucose production via protein kinase C zeta-dependent insulin receptor substrate-1 phosphorylation in HepG2 cells and mouse liver. Yeungnam Univ. J. Med. 36 (1), 26–35.
de Kloet, A.D., Krause, E.G., Woods, S.C., 2010. The renin angiotensin system and the metabolic syndrome. Physiol. Behav. 100 (5), 525–534.
Di Pasqua, L.G., et al., 2022. Detailed molecular mechanisms involved in drug-induced non-alcoholic fatty liver disease and non-alcoholic steatohepatitis: an update. Biomedicines 10 (1).
Dias-Peixoto, M.F., et al., 2012. The cardiac expression of Mas receptor is responsive to different physiological and pathological stimuli. Peptides 35 (2), 196–201.
Diep, Q.N., et al., 2002. Structure, endothelial function, cell growth, and inflammation in blood vessels of angiotensin II-infused rats: role of peroxisome proliferator-activated receptor-gamma. Circulation 105 (19), 2296–2302.
Dixon, J.B., Bhathal, P.S., O'Brien, P.E., 2001. Nonalcoholic fatty liver disease: predictors of nonalcoholic steatohepatitis and liver fibrosis in the severely obese. Gastroenterology 121 (1), 91–100.
Echeverria-Rodriguez, O., Del Valle-Mondragon, L., Hong, E., 2014. Angiotensin 1-7 improves insulin sensitivity by increasing skeletal muscle glucose uptake in vivo. Peptides 51, 26–30.
Fattahi, M.R., et al., 2016. The prevalence of metabolic syndrome in non-alcoholic fatty liver disease; A population-based study. Middle East J. Dig. Dis. 8 (2), 131–137.
Folch, J., Lees, M., Sloane Stanley, G.H., 1957. A simple method for the isolation and purification of total lipides from animal tissues. J. Biol. Chem. 226 (1), 497–509.
Ge, X., et al., 2020. Prevalence trends in non-alcoholic fatty liver disease at the global, regional and national levels, 1990-2017: a population-based observational study. BMJ Open 10 (8), e036663.
Ghasemi, A., Zahediasl, S., 2012. Normality tests for statistical analysis: a guide for non-statisticians. Int. J. Endocrinol. Metabol. 10 (2), 486–489.
Godoy-Lugo, J.A., et al., 2021. Chronic angiotensin receptor activation promotes hepatic triacylglycerol accumulation during an acute glucose challenge in obese-insulin-resistant OLETF rats. Endocrine.
Grundy, S.M., et al., 2005. Diagnosis and management of the metabolic syndrome: an American heart association/national heart, lung, and blood institute scientific statement. Circulation 112 (17), 2735–2752.
Hanefeld, M., Ableitshauser, C., 2001. Effect of the angiotensin II receptor antagonist valsartan on lipid profile and glucose metabolism in patients with hypertension. J. Int. Med. Res. 29 (4), 270–279.
Horton, J.D., et al., 1999. Disruption of LDL receptor gene in transgenic SREBP-1a mice unmasks hyperlipidemia resulting from production of lipid-rich VLDL. J. Clin. Invest. 103 (7), 1067–1076.
Ipsen, D.H., Lykkesfeldt, J., Tveden-Nyborg, P., 2018. Molecular mechanisms of hepatic lipid accumulation in non-alcoholic fatty liver disease. Cell. Mol. Life Sci. 75 (18), 3313–3327.
Jaki, T., Wolfsegger, M.J., 2009. A theoretical framework for estimation of AUCs in complete and incomplete sampling designs. Stat. Biopharm. Res. 1 (2), 176–184.
Jiang, F., et al., 2014. Angiotensin-converting enzyme 2 and angiotensin 1-7: novel therapeutic targets. Nat. Rev. Cardiol. 11 (7), 413–426.
Kaji, K., et al., 2011. Combination treatment of angiotensin II type I receptor blocker and new oral iron chelator attenuates progression of nonalcoholic steatohepatitis in rats. Am. J. Physiol. Gastrointest. Liver Physiol. 300 (6), G1094–G1104.
Kawano, Y., Cohen, D.E., 2013. Mechanisms of hepatic triglyceride accumulation in non-alcoholic fatty liver disease. J. Gastroenterol. 48 (4), 434–441.
Knebel, B., et al., 2019. Fatty Liver Due to Increased de novo Lipogenesis: alterations in the Hepatic Peroxisomal Proteome. Front. Cell Dev. Biol. 7, 248.
Kwak, S.K., Kim, J.H., 2017. Statistical data preparation: management of missing values and outliers. Kor. J. Anesthesiol 70 (4), 407–411.
Kyvelou, S.M., et al., 2006. Effects of antihypertensive treatment with angiotensin II receptor blockers on lipid profile: an open multi-drug comparison trial. Hellenic J. Cardiol. 47 (1), 21–28.
Lambert, J.E., et al., 2014. Increased de novo lipogenesis is a distinct characteristic of individuals with nonalcoholic fatty liver disease. Gastroenterology 146 (3), 726–735.
Li, Y., et al., 2019. Increased Serum Angiotensin II Is a Risk Factor of Nonalcoholic Fatty Liver Disease: A Prospective Pilot Study, 2019. Gastroenterol Res Pract, 5647161.
Lubel, J.S., et al., 2009. Angiotensin-(1-7), an alternative metabolite of the renin-angiotensin system, is up-regulated in human liver disease and has antifibrotic activity in the bile-duct-ligated rat. Clin. Sci. (Lond.) 117 (11), 375–386.
Matthew Morris, E., et al., 2013. The role of angiotensin II in nonalcoholic steatohepatitis. Mol. Cell. Endocrinol. 378 (1–2), 29–40.
Miura, S., Karnik, S.S., Saku, K., 2011. Review: angiotensin II type 1 receptor blockers: class effects versus molecular effects. J. Renin-Angiotensin-Aldosterone Syst. JRAAS 12 (1), 1–7.
Moran, T.H., 2008. Unraveling the obesity of OLETF rats. Physiol. Behav. 94 (1), 71–78.
Moreira, C.C.L., et al., 2017. Long-term effects of angiotensin-(1-7) on lipid metabolism in the adipose tissue and liver. Peptides 92, 16–22.
Motulsky, H.J., Brown, R.E., 2006. Detecting outliers when fitting data with nonlinear regression - a new method based on robust nonlinear regression and the false discovery rate. BMC Bioinf. 7, 123.
Mukaka, M.M., 2012. Statistics corner: a guide to appropriate use of correlation coefficient in medical research. Malawi Med. J. 24 (3), 69–71.
Muoio, D.M., Newgard, C.B., 2008. Fatty acid oxidation and insulin action: when less is more. Diabetes 57 (6), 1455–1456.
Nagle, C.A., Klett, E.L., Coleman, R.A., 2009. Hepatic triacylglycerol accumulation and insulin resistance. J. Lipid Res. 50 (Suppl. l), S74–S79.

Nakamura, K., et al., 1985. Microassay for proteins on nitrocellulose filter using protein dye-staining procedure. Anal. Biochem. 148 (2), 311–319.
Neuschwander-Tetri, B.A., Caldwell, S.H., 2003. Nonalcoholic steatohepatitis: summary of an AASLD single topic conference. Hepatology 37 (5), 1202–1219.
Paschos, P., Paletas, K., 2009. Non alcoholic fatty liver disease and metabolic syndrome. Hippokratia 13 (1), 9–19.
Patel, V.B., et al., 2016. Role of the ACE2/angiotensin 1-7 Axis of the renin-angiotensin system in heart failure. Circ. Res. 118 (8), 1313–1326.
Perla, F.M., et al., 2017. The role of lipid and lipoprotein metabolism in non-alcoholic fatty liver disease. Children (Basel) 4 (6).
Peter, A., et al., 2011. Hepatic glucokinase expression is associated with lipogenesis and fatty liver in humans. J. Clin. Endocrinol. Metab. 96 (7), E1126–E1130.
Rajapaksha, I.G., et al., 2021. Update on new aspects of the renin-angiotensin system in hepatic fibrosis and portal hypertension: implications for novel therapeutic options. J. Clin. Med. 10 (4).
Ran, J., Hirano, T., Adachi, M., 2004a. Chronic ANG II infusion increases plasma triglyceride level by stimulating hepatic triglyceride production in rats. Am. J. Physiol. Endocrinol. Metab. 287 (5), E955–E961.
Ran, J., Hirano, T., Adachi, M., 2004b. Angiotensin II type 1 receptor blocker ameliorates overproduction and accumulation of triglyceride in the liver of Zucker fatty rats. Am. J. Physiol. Endocrinol. Metab. 287 (2), E227–E232.
Ran, J., Hirano, T., Adachi, M., 2005. Angiotensin II infusion increases hepatic triglyceride production via its type 2 receptor in rats. J. Hypertens. 23 (8), 1525–1530.
Reudelhuber, T.L., 2006. A place in our hearts for the lowly angiotensin 1-7 peptide? Hypertension 47 (5), 811–815.
Rodriguez, R., et al., 2018a. Angiotensin receptor and tumor necrosis factor-alpha activation contributes to glucose intolerance independent of systolic blood pressure in obese rats. Am. J. Physiol. Ren. Physiol. 315 (4), F1081–F1090.
Rodriguez, R., et al., 2018b. Chronic AT1 blockade improves glucose homeostasis in obese OLETF rats. J. Endocrinol. 237 (3), 271–284.
Rodriguez, R., et al., 2021. Chronic AT1 blockade improves hyperglycemia by decreasing adipocyte inflammation and decreasing hepatic PCK1 and G6PC1 expression in obese rats. Am. J. Physiol. Endocrinol. Metab. 321 (5), E714–E727.
Rong, X., et al., 2010. Irbesartan treatment up-regulates hepatic expression of PPARalpha and its target genes in obese Koletsky (fa(k)/fa(k)) rats: a link to amelioration of hypertriglyceridaemia. Br. J. Pharmacol. 160 (7), 1796–1807.
Sahr, A., et al., 2016. The angiotensin-(1-7)/mas Axis improves pancreatic beta-cell function in vitro and in vivo. Endocrinology 157 (12), 4677–4690.
Samuel, V.T., Shulman, G.I., 2018. Nonalcoholic fatty liver disease as a nexus of metabolic and hepatic diseases. Cell Metabol. 27 (1), 22–41.
Santos, S.H., et al., 2010. Improved lipid and glucose metabolism in transgenic rats with increased circulating angiotensin-(1-7). Arterioscler. Thromb. Vasc. Biol. 30 (5), 953–961.
Santos, S.H., et al., 2012. Increased circulating angiotensin-(1-7) protects white adipose tissue against development of a proinflammatory state stimulated by a high-fat diet. Regul. Pept. 178 (1–3), 64–70.
Song, Y.S., et al., 2013. Time course of the development of nonalcoholic Fatty liver disease in the Otsuka long-evans Tokushima Fatty rat. Gastroenterol. Res. Pract. 2013, 342648.
Sternisha, S.M., Miller, B.G., 2019. Molecular and cellular regulation of human glucokinase. Arch. Biochem. Biophys. 663, 199–213.
Sukumaran, V., et al., 2011. Cardioprotective effects of telmisartan against heart failure in rats induced by experimental autoimmune myocarditis through the modulation of angiotensin-converting enzyme-2/angiotensin 1-7/mas receptor axis. Int. J. Biol. Sci. 7 (8), 1077–1092.
Thorwald, M., et al., 2018. Angiotensin receptor blockade improves cardiac mitochondrial activity in response to an acute glucose load in obese insulin resistant rats. Redox Biol. 14, 371–378.
Villanueva, C.J., et al., 2009. Specific role for acyl CoA:Diacylglycerol acyltransferase 1 (Dgat1) in hepatic steatosis due to exogenous fatty acids. Hepatology 50 (2), 434–442.
Wei, Y., et al., 2008. Angiotensin II-induced non-alcoholic fatty liver disease is mediated by oxidative stress in transgenic TG(mRen2)27(Ren2) rats. J. Hepatol. 49 (3), 417–428.
Wilson, C.G., et al., 2016. Hepatocyte-specific disruption of CD36 attenuates fatty liver and improves insulin sensitivity in HFD-fed mice. Endocrinology 157 (2), 570–585.
Yamada, S., 2011. Pleiotropic effects of ARB in metabolic syndrome. Curr. Vasc. Pharmacol. 9 (2), 158–161.
Yen, C.L., et al., 2008. Thematic review series: glycerolipids. DGAT enzymes and triacylglycerol biosynthesis. J. Lipid Res. 49 (11), 2283–2301.
Yu, J., et al., 2018. Update on glycerol-3-phosphate acyltransferases: the roles in the development of insulin resistance. Nutr. Diabetes 8 (1), 34.